Journal of Instrumentation

Algorithms for minimization of charge sharing effects in a hybrid pixel detector taking into account hardware limitations in deep submicron technology

Jinst
PUBLISHED BY IOP PUBLISHING FOR SISSA MEDIALAB
RECEIVED: *September 27, 2012*
ACCEPTED: *November 13, 2012*
PUBLISHED: *December 18, 2012*

14th INTERNATIONAL WORKSHOP ON RADIATION IMAGING DETECTORS,
1–5 JULY 2012,
FIGUEIRA DA FOZ, PORTUGAL

Algorithms for minimization of charge sharing effects in a hybrid pixel detector taking into account hardware limitations in deep submicron technology

P. Maj,[a,1] **A. Baumbaugh,**[b] **G. Deptuch,**[b] **P. Grybos**[a] **and R. Szczygiel**[a]

[a]*AGH University of Science and Technology, Al. Mickiewicza 30, 30-059 Kraków, Poland*
[b]*Fermi National Accelerator Laboratory, Batavia, IL 60510 U.S.A.*

E-mail: piotr.maj@agh.edu.pl

ABSTRACT: Charge sharing is the main limitation of pixel detectors used in spectroscopic applications, noting that this applies to both time and amplitude/energy spectroscopy. Even though, charge sharing was the subject of many studies, there is still no ultimate solution which could be implemented in the hardware to suppress the negative effects of charge sharing. This is mainly because of strong demand on low power dissipation and small silicon area of a single pixel. The first solution of this problem was proposed by CERN and consequently it was implemented in the Medipix III chip. However, due to pixel-to-pixel threshold dispersions and some imperfections of the simplified algorithm, the hit allocation was not functioning properly. We are presenting novel algorithms which allow proper hit allocation even at the presence of charge sharing. They can be implemented in an integrated circuit using a deep submicron technology. In performed simulations, we assumed not only diffusive charge spread occurring in the course of charge drifting towards the electrodes but also limitations in the readout electronics, i.e. signal fluctuations due to noise and mismatch (gain and offsets). The simulations show that using, for example, a silicon pixel detector in the low X-ray energy range, we have been able to perform proper hit position identification and use the information from summing inter-pixel nodes for spectroscopy measurements.

KEYWORDS: Simulation methods and programs; Electronic detector readout concepts (solid-state); Front-end electronics for detector readout; Analysis and statistical methods

[1]Corresponding author.

doi:10.1088/1748-0221/7/12/C12020

2012 JINST 7 C12020

Contents

1 Introduction — Charge sharing effects and scope of this work

A typical silicon pixel detector is an array of reverse junctions implanted on a high resistivity (1–10 k$\Omega\cdot$ cm) silicon substrate 250–500 μm thick. Silicon is adequate for low X-ray energy range (usually up to 12 keV), while for medical applications high Z materials are preferred (GaAs, CZT, etc). The pixel pitch in the frontier solutions [1]–[5] is in a range from 50 to 200 μm. If an X-ray photon hits a detector in the center of the pixel area a generated charge is collected on a single detector electrode. In this case the signal in a single readout channel is proportional to the photon energy and consequently the energy of the incoming photon can be determined. In case of an X-ray photon depositing energy close to the border between pixels, the generated charge drifting towards the collection electrode can be spread between two or more neighbor pixels and then inter-pixel communication inside the readout chip is necessary to recover the information about the photon energy.

Scientists working on a hybrid pixel detector struggle to reduce the pixel size in order to obtain a better position resolution. This, however leads to an increase of charge sharing events between the neighboring pixels. Charge sharing effects degrade energy resolution of detector systems and final image quality. The charge sharing phenomena in sensors with a small pixel size can be reduced by changing the geometry of a pixel (e.g. hexagonal pixels [6]), reducing the charge collection time (by detector operation at higher bias voltages [7]) or using new detector types, like 3-D structures with electrode columns penetrating the detector bulk [8]. Negative effects of the charge sharing can also be partially suppressed in the readout chip, however such solutions require inter-pixel communication on the fly and summing of charge portions from neighbor readout channels.

This work analyzes novel algorithms which can be implemented in front-end electronics and can suppress the negative effects of the charge sharing. In our simulations we have taken into account imperfections of readout electronics, such as realistic noise together with a gain and an offset spread from pixel to pixel.

Table 1. Comparison of noise and spread of gain and offsets in counting pixel chips in submicron technology.

Chip [ref]	Medipix II [1]	Pilatus 2 [2]	XPAD3S [3]	Eiger [4]	PXD18k [5]
Technology	250 nm	250 nm	250 nm	250 nm	180 nm
Chip area [mm^2]	16.1×14.1	17.5×10.5	17.4×10.4	19.3×20.1	9.64×20
Pixel matrix	256×256	60×97	80×120	256×256	96×192
Pixel size[μm^2]	55×55	172×172	130×130	75×75	100×100
Noise [e^- rms]	141	123	127	180	168
Offset spread after trim. [e^- rms]	90	10	57	20	42

2 Simulation assumption

We have made several assumptions for the spread of the charge collected on the detector electrodes regarding the pixel size and the parameters of the readout electronics. We have assumed that an X-ray photon (tested photon energy range from 8 to 12 keV) which hits a 300 μm thick Si detector generates a charge with a density cloud given by 2D Gaussian distribution with a sigma of about 10 μm [9, 10]. The spatial resolution of our simulation is 0.5 μm. Furthermore, we have assumed that the detector with a square pixel is designed with the pixel pitch of 75 μm and the simulated detector matrix contains 8 $\times$ 8 pixels. The charge cloud is randomly deposited within the central 6 $\times$ 6 pixels array.

By analyzing different solutions of existing readout integrated circuits (working in a single photon counting mode — see table 1), we have assumed that for readout electronics, this is the possible scenario: noise in the range of 75 el. rms to 150 el. rms, offset spread from 10 or 40 el. rms, with the spread of gain is 5% on one sigma level.

Testing the algorithms, we have assumed that the information about pulse amplitudes is available from individual pixels as well as from summing nodes. Two different shapers have been used in a single pixel and in summing nodes. Because of an AC coupling at the input of summing nodes (see figure 1), the offsets from single pixels do not propagate to summing nodes (which is a significant advantage compared to solutions such as [11, 12]), and the offsets spread in summing nodes is randomized independently.

3 C8P1 algorithm

The first tested algorithm is known as C8P1 (comparing with 8 neighbours when at least 1 summing node is above a threshold) In this algorithm if the amplitude in a given summing node is above a predefined threshold V_{SUM} in all pixels which contributes to this summing node and their neighbours These pixels compare their own signals with eight surrounding neighbours (left, right, up, down and also these in the corners) [13]. Every direction has only one comparator and information is shared between pixels to assure the stability of the algorithm. Finally a single pixel is elected on condition that its signal is larger than that of all its neighbours and it has at least one of its summing

2012 JINST 7 C12020

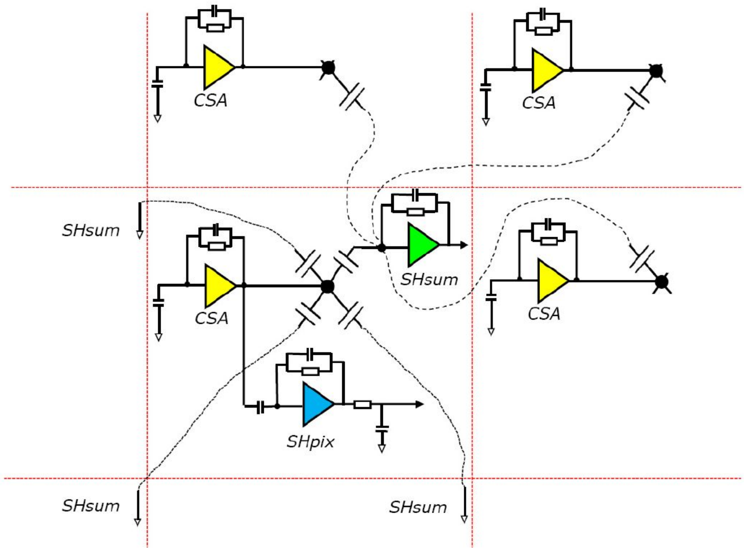

Figure 1. Summing nodes in tested algorithms.

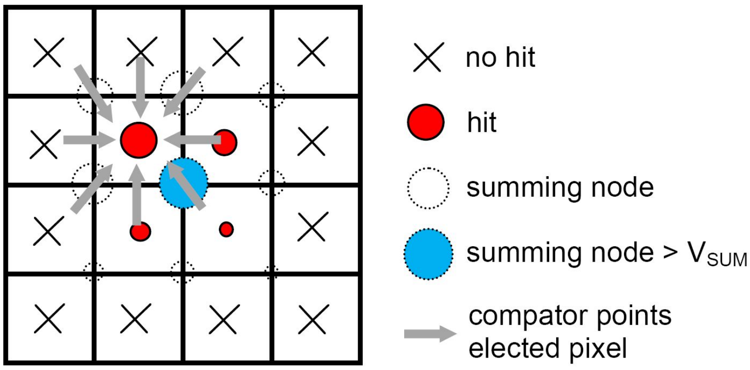

Figure 2. The idea of C8P1 algorithm.

nodes above a predefined threshold V_{SUM} – see figure 2 This algorithm has been extensively studied for different values of the input signals Q_{IN} and input parameters in the readout electronics, i.e.: noise ENC, gain variation σ_{gain}, offsets variation in discriminators $\sigma_{off-discr}$ and in comparators $\sigma_{off-comp}$. For each set of input data a 10 000 single photons hits randomly distributed were tested.

Exemplary results of our simulations are shown in figure 3 and figure 4. These pictures show the number of false hits (i.e. algorithm has elected a pixel which does not obtain a maximal charge amplitude) and missing hits (i.e. none of the pixels is elected and the photon hit is missed) as a function of the predefined threshold V_{SUM} In the presented cases the input charge is $Q_{IN} = 2200$ el. (equivalent to a photon hit of energy 8 keV in an Si detector), while other parameters are $\sigma_{gain} = 5\%$, $\sigma_{off-discr} = 20$ el. rms. The set of plots in figure 3 present cases for different values of comparator offsets $\sigma_{off-comp}$ with the assumption that ENC = 100 el. rms. As it can be seen in figure 3a (for $\sigma_{off-comp}$=0) lowering the summing node threshold leads to producing extra hits. If the summing node threshold is raised too high real hits are missed. There is, however, a reasonable range of

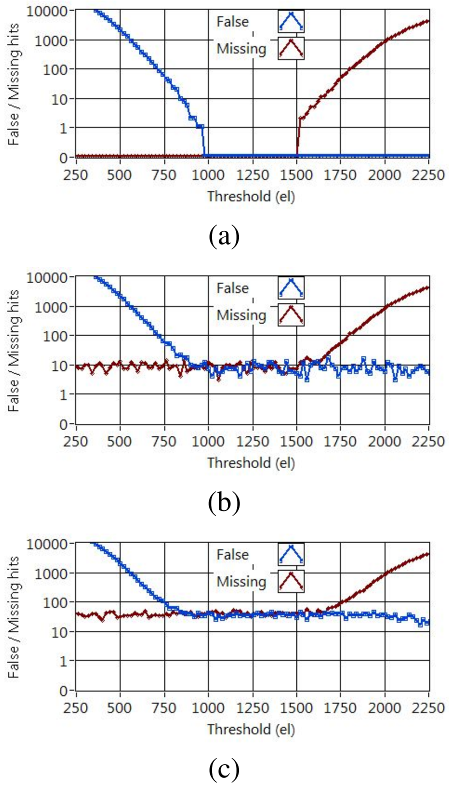

Figure 3. Test results for comparator offsets with input parameters $Q_{IN} = 2200$ el, $\sigma_{gain} = 5\%$, $\sigma_{off-discr} = 20$ el. rms, ENC = 100 el. rms and a) $\sigma_{off-comp} = 0$ el. rms, b) $\sigma_{off-comp} = 10$ el. rms, c) $\sigma_{off-comp} = 40$ el. rms.

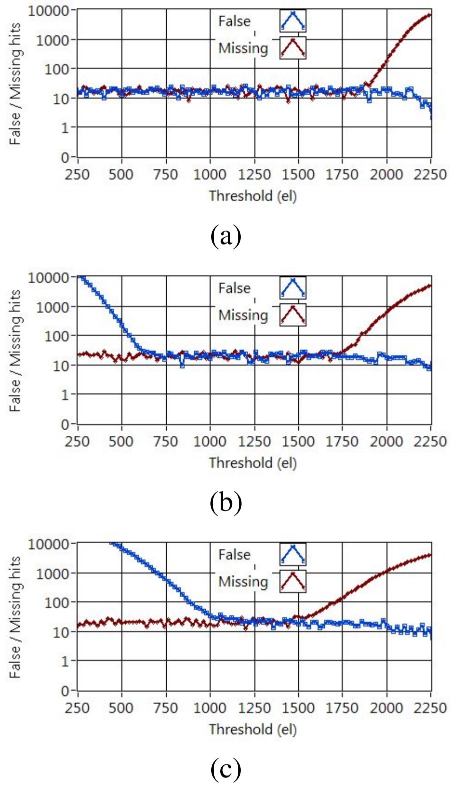

Figure 4. Test results for different noise with input parameters $Q_{IN} = 2200$ el, $\sigma_{gain} = 5\%$, $\sigma_{off-discr} = 20$ el. rms, $\sigma_{off-comp} = 20$ el. rms and a) ENC = 0 el. rms, b) ENC = 75 el. rms, c) ENC = 125 el. rms.

settings V_{SUM} (1000–1500 el.) when hit allocation is properly done (no false and no extra hits are found). Taking into account the comparator offsets (see figure 3b and figure 3c) one can see some false or missing hits in the above mentioned range of setting V_{SUM}. However their number is small (i.e. about 0.1% and 0.4% of all hits for comparator offsets 10 el. rms and 40 el. rms respectively). When the noise in the C8P1 algorithm is increasing (see figure 4) the acceptable range of setting V_{SUM} is shrinking, but for Signal to Noise Ratio (SNR) above 15 the algorithm is still working properly.

4 Pattern recognition algorithm

The second tested algorithm is called Pattern Recognition (PR). The main assumption of the presented solution is that the charge deposited inside the detector can be divided between four pixels maximum in X-ray imaging applications (this is true if the pixel area is big enough; in practice bigger than 40 μm). In the tested algorithm, we have assumed that each pixel contains a single discriminator with a configurable threshold level V_{PIX} and additionally a summing node has a discriminator (common for all four neighboring pixels) with a configurable threshold V_{SUM}. We can distinguish three main regions where the photon can hit the detector, namely: the center of the

2012 JINST 7 C12020

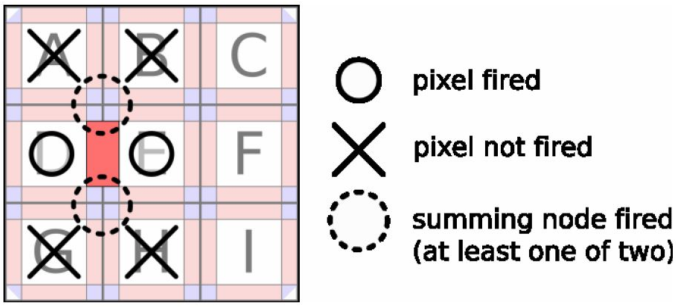

Figure 5. Photon hits the area between two pixels.

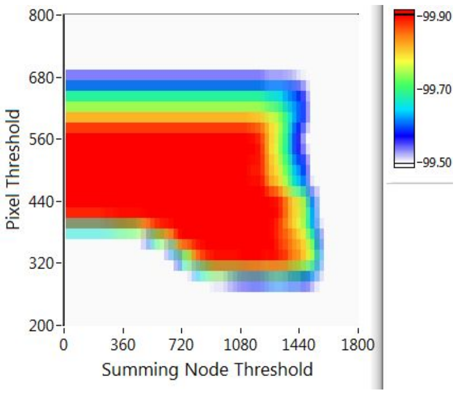

(a)

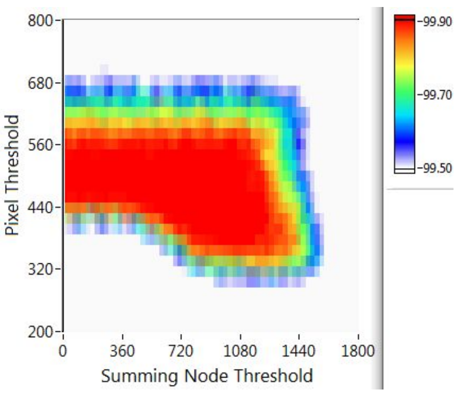

(b)

Table 2. Efficiency as a function of discriminator thresholds V_{PIX} and V_{SUM} for $Q_{IN} = 2200$ el., ENC $= 100$ el. rms and a) $\sigma_{discr} = 0$ el. rms, b) $\sigma_{discr} = 40$ el. rms.

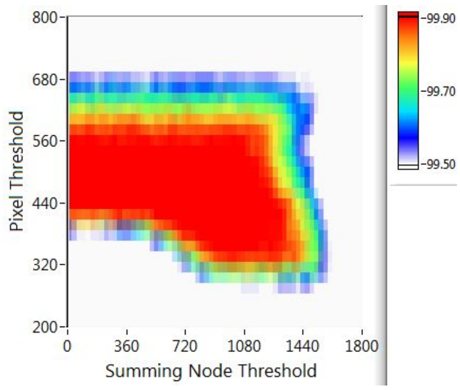

(a)

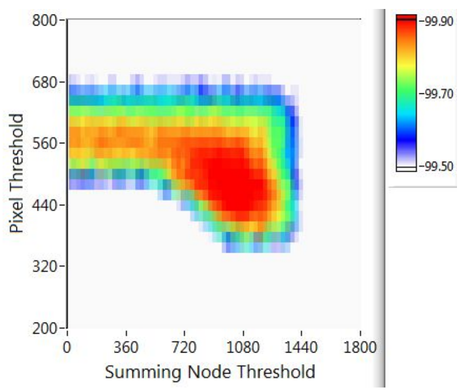

(b)

Table 3. Efficiency as a function of discriminator thresholds V_{PIX} and V_{SUM} for $Q_{IN} = 2200$ el, $\sigma_{discr} = 20$ el. and a) ENC $= 100$ el. rms, b) ENC $= 125$ el. rms.

pixel (no charge sharing), between two pixels (an example case is shown in figure 5) and between four pixels.

In simulations, we are looking for the values of discriminator thresholds V_{PIX} and V_{SUM} which guarantee a proper allocation of the hit position to the central pixel region or to one of the adjacent border regions where the charge is divided. The exemplary results of our simulations are shown in figure 2 and figure 3. The plots show which values of both thresholds (in single pixel V_{PIX} and in summing node V_{SUM}) should be set to obtain good efficiency (i.e. 99.5% or higher). figure 2 shows the efficiency for input charge $Q_{IN} = 2200$ el. and noise ENC = 100 el. rms for two different values of discriminator spread $\sigma_{off-discr}$ equal to 0 el. rms and 40 el. rms (we assume the same offset spread in pixel and in summing node). The simulations show that proper setting of the threshold in the summing node V_{SUM} extends the range of setting of threshold in pixel V_{PIX} to obtain good efficiency. Even for the discriminator spread of 40 el. rms, a reasonable range of settings V_{PIX} and V_{SUM} can be found. The influence of the noise in the tested algorithm is seen in figure 3 where two cases with ENC = 100 el. rms and ENC = 125 el. rms are shown (other parameters are set at $Q_{IN} = 2200$ el. and $\sigma_{off-discr} = 20$ el. rms). One can see that the range of allowable V_{PIX} and V_{SUM} shrinks significantly.

5 Summary

Two different algorithms C8P1 and PR have been described and tested for proper hit allocation in the presence of charge sharing. We have taken into account the imperfection of front-end electronics (noise, gain and offset spread) and analysed how they influence the process of proper hit allocation. For C8P1 the Signal to Noise Ratio of 15 is a safe limit. Additionally, we have found that comparator offsets are responsible for a very small number of false or missed hits, even in the case of the properly set discriminator threshold in the summing node. For PR, the discriminator offsets limit the range of allowable threshold settings (both for single and for summing node). In principle, the PR has also the ability to give better position information than the C8P1 because extra information is gained from adjacent hit pixels. However, our simulation shows that the PR algorithm is more sensitive to noise increase than the C8P1 one. For that reason the C8P1 was selected for hardware implementation [14].

Acknowledgments

This project at AGH University of Science and Technology was supported by National Science Center, under Contract DEC-2011/01/B/ST7/05155. Fermi National Accelerator Laboratory is operated by Fermi Research Alliance, LLC under Contract DE-AC02-07CH11359 with the U.S. Department of Energy.

References

[1] X. Llopart et al., *Medipix2: a 64-k pixel readout chip with 55-μm square elements working in single photon counting mode*, IEEE Trans. Nucl. Sci. **49** (2002) 2279.

[2] P. Kraft et al., *Characterisation and calibration of Pilatus detectors*, IEEE Trans. Nucl. Sci. **56** (2009) 758.

[3] P. Pangaud et al., *First results of XPAD3, a new photon counting chip for X-Ray CT-scanner with energy discrimination*, IEEE Nucl. Sci. Symp. Conf. Rec. **1** (2007) 14.

[4] R. Dinapoli et al., *A new family of pixel detectors for high frame rate X-ray applications*, Nucl. Instrum. Meth. **A 617** (2010) 384.

2012 JINST 7 C12020

[5] P. Maj, et al., *18k Channels single photon counting readout circuit for hybrid pixel detector*, *Nucl. Instrum. Meth.* **A 697** (2013) 32.

[6] L. Tlustos, et al., *Signal variation in high-granularity Si pixel detectors*, *IEEE Trans. Nucl. Sci.* **51** (2004) 3006.

[7] L. Rossi, P. Fischer and N. Wermes, *Pixel detectors: from fundamentals to applications*, Springer, U.S.A. (2006).

[8] C. Kenney et al., *Silicon detectors with 3-D electrode arrays: fabrication and initial test results*, *IEEE Trans. Nucl. Sci.* **46** (1999) 1224.

[9] A. Bergamaschi, et al., *Performance of single photon counting microstrip detector for strip pitches down to 10* μ*m*, *Nucl. Instr. Meth.* **A 591** (2008) 163.

[10] J. Marshal, *Theoretical analysis of the effects of charge sharing on detective quantum efficiency of single photon counting segmented silicon detectors*, 2010 *JINST* **5** P01004.

[11] R. Ballabriga, et al. *The Medipix3 prototype, a pixel readout chip working in single photon counting mode with improved spectrometric performance*, *IEEE Trans. Nucl. Sci.* **54** (2007) 1824.

[12] D. Pennicard et al., *Simulation of charge summing and threshold dispersion effects in Medipix3*, *Nucl. Instrum. Meth.* **A 636** (2011) 74.

[13] A. Baumbaugh et al., *Analysis of full charge reconstruction algorithms for X-ray pixelated detectors*, *IEEE NSS/MIC Conf. Rec.* (2011) 660.

[14] G. Deptuch et al., *A prototype pixel readout integrated circuit with reconstitution of full signals for X-ray photon science*, presented at *IEEE NSS/MIC Conference*, October 29–November 3, Disneyland Hotel, Anaheim, California, U.S.A. (2012).

2012 JINST 7 C12020